

## The Dependence between the Structural-morphological Features of SiO<sub>2</sub>/TiO<sub>2</sub> Mixes and Discharge Capacities of Lithium Power Sources

Yu.V. Yavorsky<sup>1</sup>, Ya.V. Zaulichny<sup>1</sup>, V.M. Gunko<sup>2</sup>, M.V. Karpets<sup>3</sup>, V.V. Mokliak<sup>4</sup>, A.B. Hrubiak<sup>4</sup>

<sup>1</sup> Faculty of Engineering and Physics, National Technical University of Ukraine "Igor Sikorsky Kyiv Polytechnic Institute", 35, Politechnichna St., 03056 Kyiv, Ukraine

<sup>2</sup> Chuiko Institute of Surface Chemistry, National Academy of Sciences of Ukraine, 17, General Naumov St., 03164 Kyiv, Ukraine

<sup>3</sup> Institute of Problems of Materials Science named after Frantsevich, National Academy of Sciences of Ukraine, 3, Academician Krzhizhanovsky St., 03680 Kyiv, Ukraine

<sup>4</sup> G.V. Kurdyumov Institute of Metal Physics, National Academy of Sciences of Ukraine, 36, Academician Vernadsky Blvd., 02000 Kyiv, Ukraine

(Received 19 September 2019; revised manuscript received 01 December 2019; published online 13 December 2019)

The effect of mechanical treatment at microbraker (MBT) on the structural parameters and phase composition of mixtures of silicon and titanium dioxides was studied using the method of X-ray structural analysis. Transmission electron microscopy (TEM) revealed a change in the morphological features of nanoscale powders. The change in the discharge capacities of lithium power sources (LPS) due to the mechanical treatment of the cathode material base was analyzed by galvanostatic cycling. This paper highlights the relationship between changes in structural and morphological features, electronic structure, and charge capacities of LPS. From the comparison of SEM and TEM images of mixtures of titanium and silicon oxides before and after MBT, it is established that due to MBT, the agglomerates of the initial components are simultaneously crushed with perfect mixing of oxide particles between each other and new agglomerates with a denser structure are formed. The established agglomeration is accompanied by a change in the lattice parameter  $c$  with a change in the coherent scattering regions of crystalline TiO<sub>2</sub> depending on its concentration in the mixtures. From the results of galvanostatic cycling, it is found that the charge capacity of the LPS with cathodes based on the mixture after treatment is somewhat larger compared to the charge capacity of the LPS with the cathode based on the initial mixture. The results of the analysis show that the increase of the charge capacity of the LPS with the cathode on the basic mixtures after treatment is a consequence of the redistribution of  $Sisd$ -,  $Tisd$ - and  $Op$ -valence electrons and changes of structural-morphological features in the formation of interatomic interaction between oxide particles.

**Keywords:** Mechanical treatment, Distribution of valence electrons, Coherent field, Cathode material, Lithium current sources, Point chemical analysis, Spectra.

DOI: [10.21272/jnep.11\(6\).06012](https://doi.org/10.21272/jnep.11(6).06012)

PACS numbers: 62.23.Pq, 71.20.Nr, 82.45.Fk, 82.47.Aa

### 1. INTRODUCTION

In the modern world, the pace of development of scientific and technological progress is very much dependent on new materials with predetermined unique or combined properties. However, there are many factors that affect the properties of these materials. One of the most widely used currently is the reduction of particle sizes to nanosize [1]. For example, the use of smaller and smaller particles of materials in modern microprocessors can reduce the technical process, i.e. reduce the size of the elementary component of the microprocessor (transistor, resistor, etc.). This, in turn, reduces the overall size of the microprocessor and improves its energy efficiency [2]. Factors that similarly have a tremendous influence on the material properties include morphology [3], structure [4] and electronic structure. That is, materials with a developed surface, structure and high surface energy have incredible potential for use in today's industry. It is safe to say that such materials include transition metal oxides, especially silicon and titanium oxides. The combination of the unique properties of each of them in a new nanocomposite is very likely to solve one of the challenges posed by current production to modern materials science, namely the production of cathode material for

lithium power sources (LPS) with high discharge capacity and power.

One form of very pure silica is aerosil (silica), which is amorphous and non-porous. It is characterized by high chemical resistance to the action of most chemicals and has good absorption properties, especially with polar substances. In addition to being in an amorphous state, SiO<sub>2</sub> may have a variety of morphological and structural features, namely, it may be crystalline ( $\alpha$ -quartz) [5], nanocapsules [6], nanodispersed [7], nanowires [8] or nanoporous [9]. In the search for effective cathode materials for LPS [10], special attention is paid to the study of powder oxide materials of nanometric sizes, in particular silicon dioxide. It is established that energy-intensive parameters of electrochemical power sources based on SiO<sub>2</sub> are determined not only by the presence of structural channels and the degree of dispersion of the active material [10], but also depend on the method of their production [6-8, 11].

Titanium dioxide crystallizes mainly into three different structures [12]: rutile (tetragonal), anatase (tetragonal) and brookite (rhombohedral). However, two modifications are most widely used – rutile and anatase. Both structures are mainly composed of a titanium atom surrounded by six oxygen atoms with a slight

distortion of the octahedral configuration [13]. In each structure, the two bonds between titanium atoms and octahedral oxygen atoms are slightly larger. In rutile, adjacent octahedra have one common angle along the direction (110). In the anatase, the angular exchange of octahedra in the (001) direction forms planes that are connected by edges to the octahedron planes below. In addition, titanium oxide during numerous studies on the influence of the synthesis method [14, 15], the influence of various impurities [16] on the electrochemical properties of  $\text{TiO}_2$ , as the basis of the cathode material of LPS, has been demonstrated as a very promising material in this field of use.

Therefore, based on the above it can be argued that the study of crystal-structural characteristics, morphology, electronic structure, electrochemical parameters and their changes due to a particular method of synthesis or treatment of composites based on silicon and titanium oxides is very relevant.

## 2. MATERIALS AND METHODS OF RESEARCH

### 2.1 Materials

The investigated samples of silicon and titanium oxides were synthesized at the Chuiko Institute of Surface Chemistry of NASU.

The raw materials for the pyrogenic silicon dioxide were  $\text{SiCl}_4$ , which was fed into  $\text{O}_2/\text{H}_2$  flames for hydrolysis/oxidation and the formation of nanoparticles of individual  $\text{SiO}_2$  oxides with a specific surface area of  $230 \text{ m}^2/\text{g}$  (PK300).

Titanium dioxide (anatase,  $\text{TiO}_2$ ,  $45 \text{ m}^2/\text{g}$ ) was obtained by sol-gel synthesis in aqueous medium from titanium tetrachloride, followed by purification of the product from the residues of adsorbed hydrogen chloride by calcination in a heat oven at  $400 \text{ }^\circ\text{C}$  for 3 h.

The mechanical treatment at microbraker (MBT) of  $x\text{-(SiO}_2) + y\text{-(TiO}_2)$  mixtures (where  $x$ -,  $y$ - are the mass contents of the corresponding components) was performed in a mechanical vibration mill in Ardenne (Germany). MBT occurred in a metal reactor with a diameter of 25 mm using a single metal ball with a diameter of 10 mm, at a reactor oscillation frequency of 50 Hz. All MBT samples were prepared in a vibrating mill during 5 min.

Preparation of the initial mixtures was performed by conventional stirring for 5 min, followed by stirring in a 50 Hz Ardenne mechanical vibrator (Germany) in a 25 mm diameter metal reactor using one 10 mm diameter metal ball during 3 s.

### 2.2 Methods of Research

Considering that in [17] the results of the study of changes in morphological features (investigated using SEM) and electronic structure (investigated using ultra-soft X-ray emission spectroscopy (USXES)) do not fully understand the mechanisms of change in electrochemical characteristics, it is necessary to use TEM for a more detailed examination of the morphology and a detailed analysis of the results of X-ray structural analysis, namely, changes in the the coherent-scattering region (CSR), phase composition and lattice parameters.

The studies of the morphology and structure of  $\text{SiO}_2/\text{TiO}_2$  mixtures were performed using a Selmi 125K transmission electron microscope at the KPI Institute. All the samples were applied on a copper mesh with a carbon film.

The crystalline structure of the powder mixture was studied using an Ultima IV (Rigaku, Japan) diffractometer with monochromatic  $\text{CuK}\alpha$  radiation. XRD patterns of the powder mixture were analyzed using Power Cell 2.4 program. The analysis of XRD profiles and the allocation of true physical broadening of peaks was carried out using an approximation method. The separation of the broadening effects of the XRD peaks associated with the size of the coherent-scattering region and the tensions of the second kind was carried out using the Hall-Williamson approximation. The crystallinity of the investigated powders was determined by the normalization of the integral intensity of the amorphous halo to the value of the intensity of the diffraction maximum corresponding to the completely amorphous sample with similar composition.

The study of the electrochemical properties was carried out in the laboratories of the Vasyl Stefanyk Precarpathian National University. One of the most important electrochemical properties is cyclicity and charge/discharge capacity. After all, the longevity of use and the cost-effectiveness of manufacturing LPS will depend on these parameters.

The basic scheme of LPS (Fig. 1) includes [18]:

- anode (lithium metal or material containing lithium ions);
- cathode (material into which channels of crystalline structure are intercalated by  $\text{Li}^+$  ions);
- electrolyte (lithium-containing liquid, solid or gel material with ionic type of conductivity).

When the circuit closes, under the action of the potential difference between the anode and the cathode, the element discharge process takes place – the lithium ions move from the anode to the cathode and are intercalated (introduced) into the structure of the latter. In the process of charge, the deintercalation (extraction) of lithium ions from the cathode material (CM) and their transfer to the anode occurs under the action of an electric field.

Charge capacities studies were conducted on a universal stand to investigate the intercalation properties

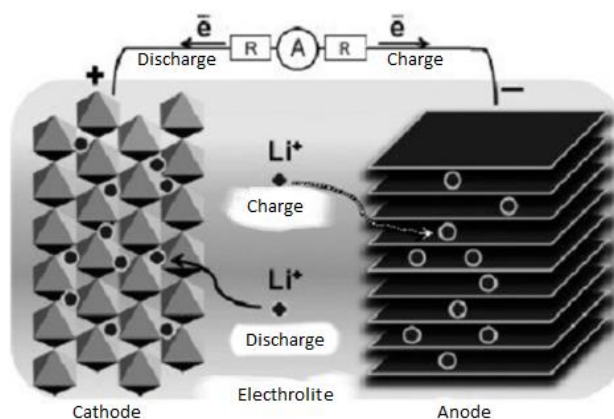


Fig. 1 – The basic scheme of LPS

of TiONiT P2.00 in galvanostatic mode; all parameters, at which the cyclization was performed, were set on a computer connected to the instrument when using the MultiCycle software. The voltage range was chosen taking into account the chemical potentials of the cathode and the anode material (metallic Li). In determining the optimal charge/discharge current, a current of 0.1 was selected from the theoretically calculated specific capacitance of the LPS (0.1 C). The results were processed using Microsoft Excel and OriginPRO.

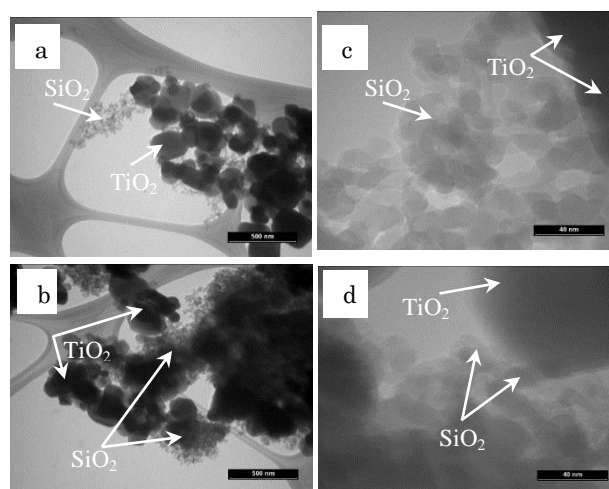
### 3. RESULTS AND DISCUSSION

When considering the SEM images of the initial components of the mixtures before and after the MBT [19], it was found that due to MBT of SiO<sub>2</sub>, little agglomeration occurs, whereas MBT of TiO<sub>2</sub> leads to a more significant merging of the oxide particles with each other. As indicated, this is most likely because titanium oxide consists of two phases (rutile and anatase), which have different chemical potentials [19].

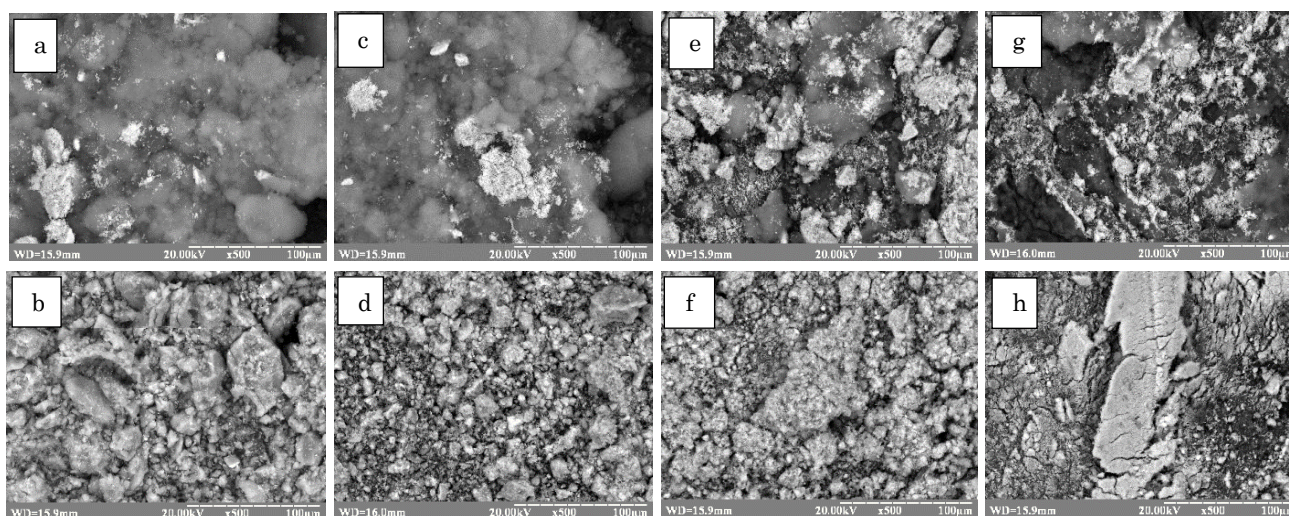
Consider the comparison of SEM images of  $x\text{-SiO}_2 + y\text{-TiO}_2$  mixtures before and after MBT [17], in which the difference of chemical potentials is much larger. At the image of the initial 0.8 SiO<sub>2</sub> + 0.2 TiO<sub>2</sub> mixture (Fig. 2), we can see that SiO<sub>2</sub> nanoparticles and TiO<sub>2</sub> particles (0.5-2 μm) are distributed throughout the volume without forming any definite structure. At the same time, after MBT of the mixture, the agglomerates of 20-50 microns with a pronounced structure are formed. Similar agglomeration is observed with the concentration of silicon oxide of 60 and 40 wt. % Increasing content of TiO<sub>2</sub> to 40 wt. % shows that the density of filling the space between the agglomerates of the particles increases as well as the density of the agglomerates themselves whose dimensions are in the region of 5-20 microns. The density between the agglomerates increases with increasing TiO<sub>2</sub> bounding. In addition, when the maximum con-

tent of TiO<sub>2</sub> occurs, high-density agglomerates of 50-150 μm in size are the centers of consolidation, which is likely to be a small number of SiO<sub>2</sub> nanoparticles. It should be noted that with increasing TiO<sub>2</sub> concentration, the agglomerates become smaller even than the accumulation of titanium dioxide in the initial mixtures.

For more detailed investigation of the nanoparticle consolidation, we conducted TEM studies of the mixture 0.8 SiO<sub>2</sub> + 0.2 TiO<sub>2</sub> before and after MBT (Fig. 3) at different magnifications. Comparison of the TEM images of the original mixtures shows that the SiO<sub>2</sub> (7-10 nm) and TiO<sub>2</sub> (50-100 and 200-300 nm) nanoparticles are grouped separately from each other. At the same time, after MBT, the SiO<sub>2</sub> and TiO<sub>2</sub> nanoparticles are to some extent interconnected into agglomerates with a denser structure and larger than 1 μm in size. In this case, we can see the incorporation of smaller SiO<sub>2</sub> nanoparticles into TiO<sub>2</sub> nanoparticles (Fig. 3d).



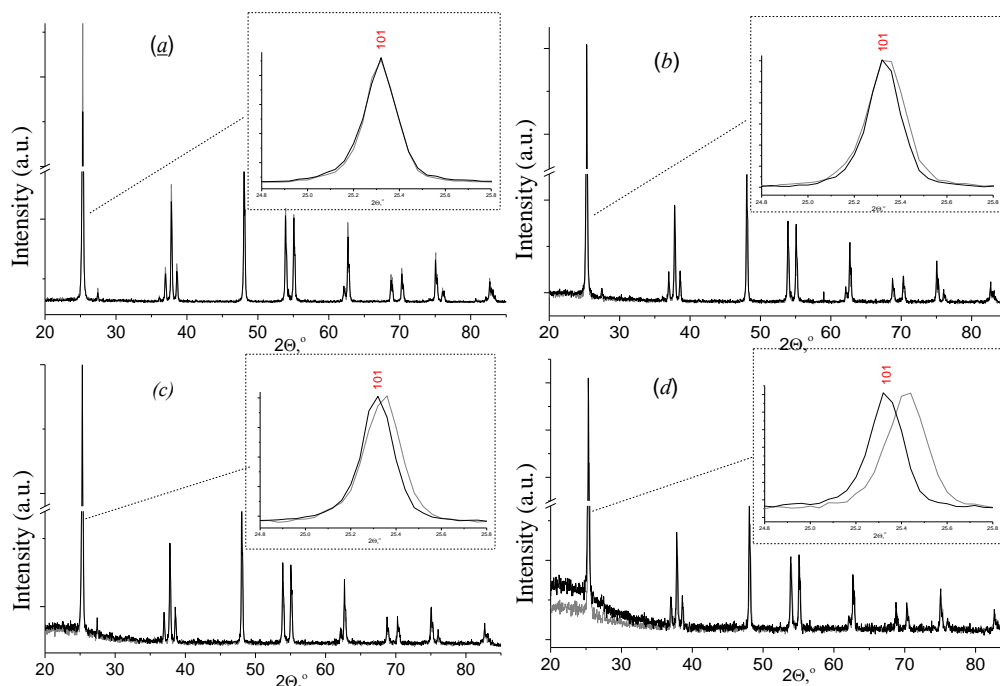
**Fig. 3** – TEM images of 0.8 SiO<sub>2</sub> + 0.2 TiO<sub>2</sub> before (a, c) and after (b, d) MBT



**Fig. 2** – SEM images of nanocomposites with different mass ratios of the components before (a, c, e, g) and after (b, d, f, h) MBT at magnification 500 times. (a, b) 0.8 SiO<sub>2</sub> + 0.2 TiO<sub>2</sub>; (c, d) 0.6 SiO<sub>2</sub> + 0.4 TiO<sub>2</sub>; (e, f) 0.4 SiO<sub>2</sub> + 0.6 TiO<sub>2</sub> and (g, h) 0.1 SiO<sub>2</sub> + 0.9 TiO<sub>2</sub>

**Table 1** – Phase composition, CSR sizes ( $D$ ), the lattice parameters ( $a$ ,  $c$ ) and changes in the lattice parameters ( $\Delta$ ) in the initial and MBT mixtures of  $x$ -SiO<sub>2</sub> +  $y$ -TiO<sub>2</sub> with different precursor mass ratios

Sample	Phase composition, mass. %	$D$ , nm	$\Delta D$ , nm	Lattice parameter	Size, nm	$\Delta$ , nm
0.1 SiO <sub>2</sub> + 0.9 TiO <sub>2</sub>	Rutile – 1.6	88	+ 2	$a$	0.3784	$\Delta a =$
	Anatase – 98.4			$c$	0.9511	$- 0.0001$
0.1 SiO <sub>2</sub> /0.9 TiO <sub>2</sub> MBT	Rutile – 1.9	90		$a$	0.3783	$\Delta c =$
	Anatase – 98.1			$c$	0.9510	$- 0.0001$
0.4 SiO <sub>2</sub> + 0.6 TiO <sub>2</sub>	Rutile – 0.9	85	+ 9	$a$	0.3786	$\Delta a =$
	Anatase – 99.1			$c$	0.9518	$- 0.0002$
0.4 SiO <sub>2</sub> + 0.6 TiO <sub>2</sub> MBT	Rutile – 0.9	94		$a$	0.3784	$\Delta c =$
	Anatase – 99.1			$c$	0.9512	$- 0.0006$
0,6SiO <sub>2</sub> +0,4TiO <sub>2</sub>	Rutile – 0.8	86	+ 16	$a$	0.3787	$\Delta a =$
	Anatase – 99.2			$c$	0.9518	$- 0.0002$
0,6SiO <sub>2</sub> +0,4TiO <sub>2</sub> MBT	Rutile – 0.4	102		$a$	0.3785	$\Delta c =$
	Anatase – 99.6			$c$	0.9512	$- 0.0006$
0.8 SiO <sub>2</sub> + 0.2 TiO <sub>2</sub>	Rutile – 0.3	84	+ 14	$a$	0.3788	$\Delta a =$
	Anatase – 99.7			$c$	0.9523	$- 0.0003$
0.8 SiO <sub>2</sub> + 0.2 TiO <sub>2</sub> MBT	Rutile – 0.1	98		$a$	0.3785	$\Delta c =$
	Anatase – 99.9			$c$	0.9515	$- 0.0008$
Error of experiment	$\pm 5$		$\pm 2$	$x$	0.0003	0.0003

**Fig. 4** – X-ray diffraction pattern of the initial (gray line) and MBT (black line) mixtures: a – 0.1 SiO<sub>2</sub> + 0.9 TiO<sub>2</sub>, b – 0.4 SiO<sub>2</sub> + 0.6 TiO<sub>2</sub>, c – 0.6 SiO<sub>2</sub> + 0.4 TiO<sub>2</sub>, d – 0.8 SiO<sub>2</sub> + 0.2 TiO<sub>2</sub>

From the results of X-ray diffraction analysis of SiO<sub>2</sub> and TiO<sub>2</sub> before and after MBT [19], it was found that the crystal-structural parameters of the original precursors did not change due to treatment. At the same time, due to MBT of mixtures with different component ratios (Fig. 4), we can see narrowing and displacement toward smaller angles of anatase diffraction peak. The CSR based on these data were found to be increased after MBT of mixtures and increasing with increasing content in the mixtures (Table 1). In addition, the determination of the crystal lattice param-

eters (Table 1) showed that the parameter "c" due to MBT decreases with increasing SiO<sub>2</sub> content by 0.0006-0.0008 nm. At the same time, the phase composition of the mixture due to the shock-vibration treatment does not change (Table 1). The increase in the CSR due to MBT and the decrease in the lattice parameters together with the formation of agglomerates are most likely due to the occurrence of interatomic interaction between the components in the process of MBT.

A study of the effect of MBT on the change in the distribution of  $Op$ -,  $Sisd$ -, and  $Tisd$ -valence electrons, which

are reflected by  $OK\alpha$ -,  $SiLa$ -, and  $TiLa$ -emission bands, obtained by USXES [17]. From the results of the analysis, it was found that due to MBT, the intensity of the high-energy region of  $SiLa$ - and  $TiLa$ -bands decreases, while at the same time the intensity of the  $OK\alpha$ -band in the energy region corresponding to  $Op_n$ -levels increases. This may indicate that the electron orbitals of oxygen, silicon, and titanium overlap in the process of high-pressure MBT. As a result, further splitting of  $Op_n$ -levels occurs and their electrons are transferred from the  $sd$ -states of titanium and silicon. That is, based on the results of SEM, TEM, XRD and USXES, it is safe to say that an interatomic interaction is formed between the oxide nanoparticles. Therefore, let us consider how the charge capacities of the LPS change as a result of such changes in the structural-morphological and electron-structural parameters.

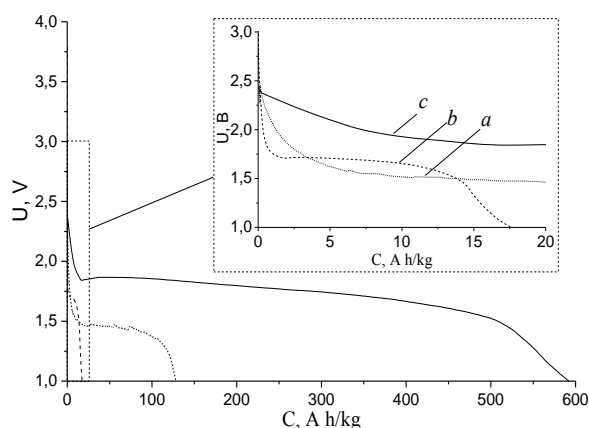


**Fig. 5** – Comparison of discharge curves of LPS with cathodes based on: 1 – 0.1  $SiO_2$  + 0.9  $TiO_2$ ; 2 – 0.4  $SiO_2$  + 0.6  $TiO_2$ ; 3 – 0.8  $SiO_2$  + 0.2  $TiO_2$

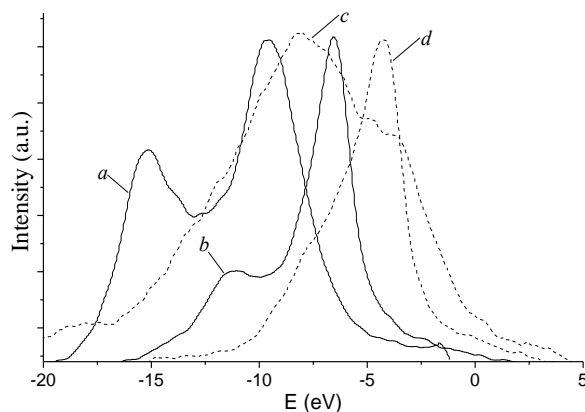


**Fig. 6** – Comparison of combined in a single energy scale 1- $SiLa$ - and 2- $OK\alpha$ -spectra from initial  $SiO_2$ , 3- $TiLa$  and 4- $OK\alpha$ -spectra from initial  $TiO_2$

First, we analyze the effect of the change in the mass ratio of oxides in the mixture. From Fig. 5 we can see that the voltage of the first cycle of LPS with a cathode based on the initial mixture with a maximum concentration of silicon dioxide is 1.8 V. With increasing concentration of  $TiO_2$  in the mixture of cathode material of LPS to 60 and 90 wt. %, the voltage of the first cycle decreases to 1.7 V and 1.46 V, respectively. In addition, this figure shows that the shape of the first discharge curves is similar for all composites.

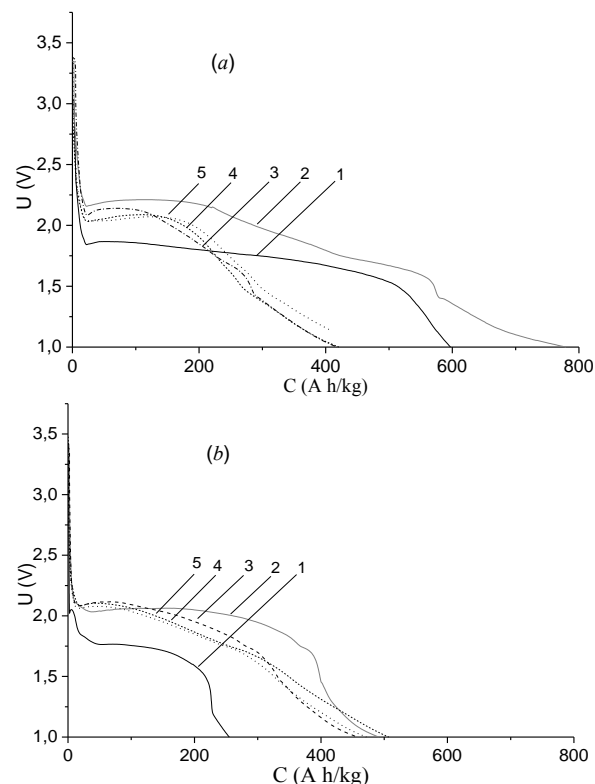


**Fig. 7** – Discharge curves of initial (a) and MBT (b) 0.8  $SiO_2$  + 0.2  $TiO_2$  mixtures: 1-5 – number of cycle

It is common knowledge that the working voltage of the LPS is determined by the difference between the chemical potential of the anode material, which is served by metallic Li ( $-3eV$ ), and the chemical potential of the electrode material. The chemical potential is determined by the position of the Fermi level in the cathode composite material. Therefore, the decrease in the working potential difference with increasing titanium dioxide concentration is associated with a shift of the valence band to the high-energy side, as a consequence of the corresponding superposition of the  $SiO_2$   $Op$ - and  $Sisd$ -states and the higher  $TiO_2$   $Op$ - and  $Sisd$ -states (Fig. 6).

From Fig. 7a, we can see that discharge LPS with a cathode based on initial 0.8  $SiO_2$  + 0.2  $TiO_2$  mixture occurs at different voltage decay to the value of 1.84 V. Then, voltage increases to the value of 1.87 V with stabilization of voltage at this level to a specific capacitance of 500 A-h/kg and a slight decrease in voltage. During the next cycles, the LPS sharply discharges to 2.17 V and subsequently the voltage increases to 2.21 V and discharges with significant voltage jumps during  $\Delta C = 200$  A-h/kg. Such jumps are the result of the interaction between  $Li^+$  and  $O^-$  and creation of various oxide groups on the surface of the cathode material. This further prevents inter- and deintercalation of lithium ions into the structure of the cathode material, which is confirmed by a sharp decrease in the charge capacity of the LPS to 400 A-h/kg during the next cycling.

At the same time, LPS with a cathode based on MBT mixture of 0.8  $SiO_2$  + 0.2  $TiO_2$  at the first discharge cycle have sharp drop to a voltage of 2 V in a

very narrow section  $\Delta C = 18$  A·h/kg. Then the discharge occurs more evenly at a voltage of 1.76 V and slight change in the potential difference up to 212 A·h/kg. The smaller initial discharge capacity of the LPS cathode based on the MBT mixture is a consequence of the formation of an interatomic interaction between the nanoparticles of both oxides and the formation of agglomerates with a pronounced structure (Fig. 2). In the next cycle, the operating voltage is increased to 2.07 V, the charge capacity is increased to 483 A·h/kg, and the power is 2.13 times higher. However, unlike LPS with the cathode based on the initial mixture, the next cycling stabilizes the charge capacity with a slight decrease in power, 0.93 times, relative to the second cycle. Such stabilization is a consequence of the increase of the bound charge state of oxygen due to MBT of mixture and the transfer of  $Sisd$ - electrons into  $Op_n$ -bound oxide states. As a result, it is much harder for  $Li^+$  ions to detach electrons from oxygen anions and recombine in the cathode material to a neutral state. When  $Li^+$  combines with the oxygen ions, it forms  $LiO$  films at the boundaries of the cathode nanoparticles.

By increasing the concentration of  $TiO_2$  in the mixture to 60 wt. %, there is a significant decrease in the charge capacity of the LPS with the cathode based on it (Fig. 8), namely, the initial charge capacity of the LPS is only 18 A·h/kg. At the same time, in the LPS with a cathode after MBT of 0.4  $SiO_2$  + 0.6  $TiO_2$  mixture the charge capacity is 57 A·h/kg, which is almost three times larger than the initial capacity of the LPS with a cathode based on the initial mixture. Such a sharp change in the charge capacity of the LPS based on the initial mixture is reduced by increasing concentration of titanium oxide. It should be noted that due to MBT, the oxygen charge has increasing population of electrons at  $Op_n$ -states as a

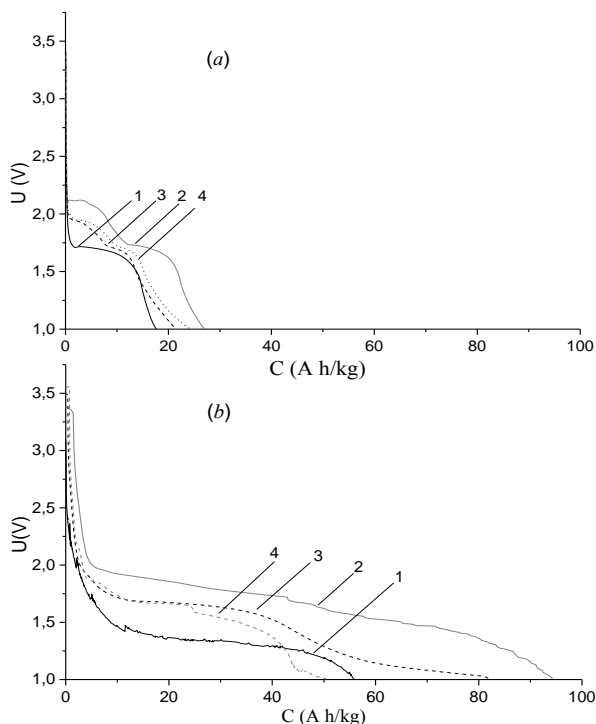


**Fig. 8** – Discharge capacity of initial (a) and after MBT (b) 0.4  $SiO_2$  + 0.6  $TiO_2$  mixtures: 1-4 – number of cycle

result of the transfer of  $s$ - and  $d$ -electrons mostly from titanium. An increase in the charge state of oxygen indicates the formation of an interatomic interaction between  $SiO_2$  and  $TiO_2$  surface atoms, which obviously contributes to the greater penetration of lithium ions into structural defects and pores of the cathode material of LPS. The next cycle of these LPS increases the charge capacity twice, but the shape of the discharge curves indicates the formation of oxide groups on the surface of the cathode material, resulting in a decrease in the charge capacity at the next cycling (Fig. 8).

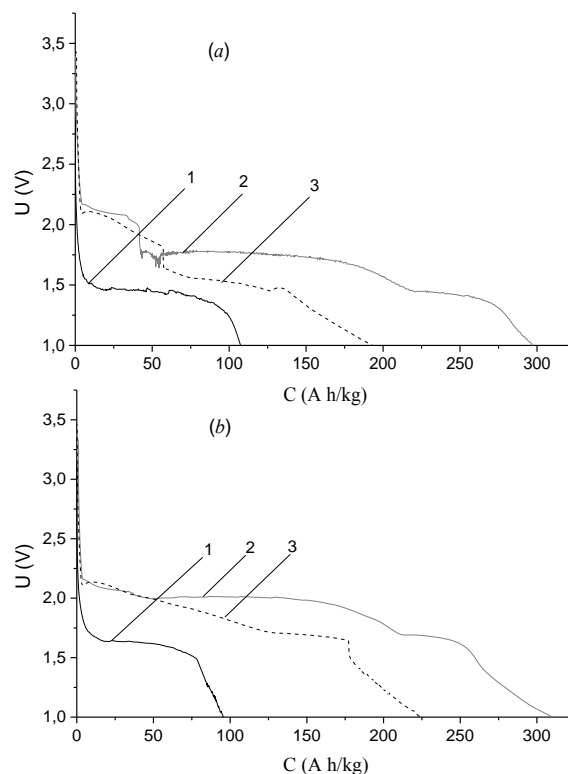


**Fig. 9** – Discharge curves of initial (a) and MBT (b) 0.1  $SiO_2$  + 0.9  $TiO_2$  mixtures: 1-3 – number of cycle

With increasing concentration of titanium dioxide in the mixture to a maximum value of 90 wt. %, the charge capacitance of the LPS with the cathode based on the initial and MBT mixture is near 100 A·h/kg (Fig. 9). In subsequent cycling, the capacitance of both LPS is almost the same, but the power of the LPS with the cathode based on the MBT mixture is much higher. The power of LPS with cathode based on MBT mixture 0.1  $SiO_2$  + 0.9  $TiO_2$  increased due to the change in the nature of the interaction between  $SiO_2$  and  $TiO_2$  nanoparticles. In this case, the increase of the charge state of oxygen is due to the transfer of electrons from high-energy  $Tisd$ -states to the  $p_n$ -states of oxygen. This is slightly different from the mixture with maximum concentration of silica dioxide, because we saw transfer of electrons from  $Sisd$ -states to the  $Op$ -states in the mixture 0.8  $SiO_2$  + 0.2  $TiO_2$ . At the same time, the shape of the discharge curves of both LPS during the second and third discharge cycles testifies to the formation of oxides, which are most likely to be accompanied by a further decrease in the charge capacity of the LPS during next cycling.

#### 4. CONCLUSIONS

The high local pressures that accompany the process of treatment at microbracer contribute to the interatomic interaction between surface nanoparticles of SiO<sub>2</sub> and TiO<sub>2</sub>. As a result of that we can see changes in the morphology and structure of nanocomposites, namely the formation of agglomerates.

Increasing density of bound electrons at  $O_{p_{II}}$ -levels due to transferring electrons from silicon reduces the recombination ability of Li<sup>+</sup> ions, which prevents the formation of LiO oxide film around the nanoparticles. As a result, the growth of the charge capacitance of the LPS, with the cathode based on the mixture after MBT 0.8 SiO<sub>2</sub> + 0.2 TiO<sub>2</sub>, after cycling are stabilized.

With increasing concentration of TiO<sub>2</sub> to 53 mol. % the charge capacity of the LPS, based on the initial mixture, is reduced by increasing the concentration of

titanium dioxide. At the same time, the charge capacity of the LPS, based on the mixture after MBT, increases due to the formation of interatomic interaction between the surface atoms of titanium and silicon oxides. As a result of the increase in the density of  $O_{p_{II}}$ -coupled electrons due to their transfer from titanium  $sd$ -states, the lithium ions penetrate into the structural defects and pores of the cathode material of the LPS.

#### ACKNOWLEDGEMENTS

The authors are grateful to the workers of Laboratory of Electron Microscopic Investigation of the Faculty of Engineering and Physics of the Igor Sikorsky Kyiv Polytechnic Institute for their assistance in obtaining and analyzing images of scanning electron microscopy of the studied samples.

#### REFERENCES

1. Г.П. Ковтун, А.А. Веревкин, *Наноматеріалы: технології і матеріалознавство* (Харьков: ННЦ ХФТИ: 2010). (G.P. Kovtun, A.A. Verevkin, *Nanomaterialy: tekhnologii i materialovedeniye* (Khar'kov: NNTS KHFTI: 2010)) [In Russian].
2. James Niemann, *Electrical Measurements on Nanoscale Materials* (2005).
3. Selvan Mohan, Juliska Princz, Banu Ormeci, Maria C. DeRosa, *Nanomaterials* **9**(9), 1258 (2019).
4. Hui Xia, Michael Z. Hu, Ying Shirley Meng, Jianping Xie, Xiangyu Zhao, *J. Nanomater.* **2014**, Article ID 675859 (2014).
5. Nan Yan, Fang Wang, Hao Zhong, et al., *Sci. Rep.* **3**, 1568 (2013).
6. Yuefei Zhang, Yujie Li, Zhenyu Wang, Kejie Zhao, *Nano Lett.* **10**, 1021 (2014).
7. J. Zhang, L.B. Chen, C.C. Li, T.H. Wang, *Appl. Phys. Lett.* **93**, 264102 (2008).
8. Xifei Li, Abirami Dhanabalan, Xiangbo Meng, et al., *Micropor. Mesopor. Mater.* **151**, 488 (2012).
9. C. Cannas, D. Gatteschi, A. Musini, et al., *J. Phys. Chem. B* **102**, 7721 (1998).
10. I.F. Myronyuk, V.V. Lobanov, B.K. Ostafiychuk, et al., *Phys. Chem Solid State* **2** No 4, 653 (2001) [In Ukrainian].
11. Yurong Ren, Hengma Wei, Xiaobing Huang, Jianning Ding, *Int. J. Electrochem. Sci.* **9**, 7784 (2014).
12. L.S. Dubrovinsky, N.A. Dubrovinskaia, V. Swamy, et al., *Nature* **410**, 653 (2001).
13. V.M. Gun'ko, V.I. Zarko, R. Leboda, E. Chibowski, *Adv. Colloid Interface Sci.* **91**, 1 (2001).
14. Biao Han, Young-Woo Lee, Si-Jin Kim, et al., *Int. J. Electrochem. Sci.* **8**, 8264 (2013).
15. Ming-Che Yang, Yang-Yao Lee, Bo Xu, et al., *J. Power Sources* **207**, 166 (2012).
16. Beata Kurc, Teofil Jesionowski. Beata Kurc, *J. Solid State Electrochem.* **19**, 1427 (2014).
17. Ю.В. Яворський, Я.В. Зауличний, В.Я. Ільків, О.І. Дудка, А.П. Чмерук, В.І. Зарко, М.В. Карпець, *Фізична інженерія поверхні* **13** № 3, 371 (2015) (Yu.V. Yavors'kyu, Ya.V. Zaulichnyy, V.Ya. Il'kiv, O.I. Dudka, A.P. Chmeruk, V.I. Zarko, M.V. Karpets', *Fizychna inzheneriya poverkhni* **13** No 3, 371 (2015)) [In Ukrainian].
18. В.О. Коцюбинський, В.Л. Челядин, В.В. Мокляк та ін., *Фізика і хімія твердого тіла* **11** № 2, 484 (2010) (V.O. Kotsyubyns'kyu, V.L. Chelyadyn, V.V. Moklyak, et al., *Phys. Chem. Solid State* **11** No 2, 484 (2010)) [In Ukrainian].
19. Yu.V. Yavorsky, Ya.V. Zaulichny, V.M. Gunko, M.V. Karpets, *J. Nano- Electron. Phys.* **10** No 6, 06005 (2018).

#### Залежність між структурно-морфологічними особливостями сумішей SiO<sub>2</sub>/TiO<sub>2</sub> та розрядними ємностями літєвих джерел струму

Ю.В. Яворський<sup>1</sup>, Я.В. Зауличний<sup>1</sup>, В.М. Гунько<sup>2</sup>, М.В. Карпець<sup>2</sup>, В.В. Мокляк<sup>4</sup>, А.Б. Груб'як<sup>4</sup>

<sup>1</sup> Інженерно-фізичний факультет, Національний технічний університет України «Київський політехнічний інститут імені Ігоря Сікорського», вул. Політехнічна, 35, 03056 Київ, Україна

<sup>2</sup> Інститут хімії поверхні імені О.О. Чуйка, Національна академія наук України, вул. Генерала Наумова, 17, 03164 Київ, Україна

<sup>3</sup> Інститут проблем матеріалознавства імені Францевича, Національна академія наук України, вул. Академіка Кржижанівського, 3, 03680 Київ, Україна

<sup>4</sup> Інститут металофізики імені Г.В. Курдюмова, Національна академія наук України, бульв. Академіка Вернадського, 36, 02000 Київ, Україна

Використовуючи метод рентгеноструктурного аналізу було вивчено вплив ударно-вібраційної обробки (УВО) на структурні параметри та фазовий склад сумішей діоксидів кремнію та титану. За допомогою методу трансмісійної електронної мікроскопії (ТЕМ) встановлена зміна морфологічних особливостей нанорозмірних порошоків. Методом гальваностатичного циклювання проаналізовано зміну зарядових ємностей літєвих джерел струму (ЛДС) внаслідок УВО основи катодного матеріалу. У да-

ній роботі висвітлена залежність між зміною структурно-морфологічних особливостей, електронної структури та зарядовими емностями ЛДС. Із порівняння СЕМ та ТЕМ зображень сумішей оксидів титану та кремнію до та після УВО встановлено, що внаслідок УВО відбувається одночасне подрібнення конгломератів вихідних компонент з подальшим рівномірним розподілом частинок оксидів один між одним та утворення нових агломератів з більш щільною структурою. Встановлена агломерація супроводжується зміною параметра ґратки с зміною областей когерентного розсіювання кристалічного  $\text{TiO}_2$  в залежності від концентрації його в суміші. З результатів гальваностатичного циклювання встановлено, що зарядова емність ЛДС з катодами на основі суміші після УВО є дещо більшою у порівнянні із зарядовою емністю ЛДС з катодом на основі вихідної суміші. З результатів аналізу встановлено, що збільшення зарядової емності ЛДС з катодом на основі сумішей після УВО є наслідком перерозподілу  $\text{Si}3d$ -,  $\text{Ti}3d$ - та  $\text{O}p$ -валентних електронів та зміни структурно-морфологічних особливостей при утворенні міжатомної взаємодії між наночастинками оксидів.

**Ключові слова:** Ударно-вібраційна обробка (УВО), Трансмісійна електронна мікроскопія (ТЕМ), Рентгеноструктурний аналіз, Скануюча електронна мікроскопія (СЕМ), Ультра м'яка рентгенівська емісійна спектроскопія (УМРЕС), Розподіл валентних електронів, Область когерентного розсіювання, Фазовий склад, Катодний матеріал, Точковий хімічний аналіз,  $\text{Si}L\alpha$ -,  $\text{Ti}L\alpha$ -,  $\text{OK}\alpha$ -спектри.